Two-Step Tumor-Targeting Therapy *via* Integrating Metabolic Lipid-Engineering with *in situ* Click Chemistry

Guihong Lu[#a], Liping Zuo[#a], Jinfeng Zhang[a], Houshun Zhu[a], Wanru Zhuang[a], Wei Wei[b], Hai-Yan Xie*[a]

a School of Life Science, Beijing Institute of Technology, No.5 South Zhong Guan Cun Street, Beijing 100081, China
b State Key Laboratory of Biochemical Engineering, Institute of Process Engineering, Chinese Academy of Sciences, 1 North 2nd Street, Zhong Guan Cun, Beijing 100190, China

Experimental Section

Materials and Reagents. Dulbecco's modified Eagle's medium (DMEM) and fetal bovine serum (FBS) were obtained from Gibco Life Technologies (AG, Switzerland). Trypsin-EDTA, penicillin-streptomycin and Hoechst 33342 were purchased from Life Technologies. Calcein-AM and propidium iodide (PI) were obtained from Invitrogen (USA). NHS-PEG_4-DBCO, Azide-Flour 488 and DBCO-Flour 525 were purchased from Click Chemistry Tools (Scottsdale, AZ). ICG and other materials were purchased from J&K Scientific Ltd.

Cell Culture. The MDA-MB-231 breast tumor cells were purchased from Peking Union Medical College Hospital and cultured in DMEM with 10% FBS and 1% (v/v) penicillin-streptomycin. The cells were incubated in a 5% CO_2 incubator at 37 °C. Red blood cells were obtained from KM mice (Vital River Laboratories).

Animals and Tumor Model. Four-week-old Balb/c nude mice were purchased from Vital River Laboratories (Beijing, China). All animal procedures were performed in accordance with the Regulations for Care and Use of Laboratory Animals and Guideline for Ethical Review of Animal (China, GB/T 35892-2018) and approved by the Animal Ethics Committee of the Institute of Process Engineering (approval ID: IPEAECA2019094). A breast cancer model was established by subcutaneously inoculating MDA-MB-231 cells (1×10^7 cells) into the flank of Balb/c nude mice. Tumor volume was calculated as (tumor length) × $(\text{tumor width})^2/2$.

Preparation and Characterization of RBCG. Whole blood was centrifuged at 3000 rpm for 8 min at 4 °C after obtained from KM mice (6-8 w), then the serum and the buffy coat were carefully removed. The resulting packed RBCs were washed with cold PBS for three times and suspended in 0.25× PBS in an ice bath for 40 min, followed by centrifuging at 9000 rpm for 10 min. The pink RBC ghosts were collected after the hemoglobin was removed. The resulting RBC ghosts were verified using microscopy.

After that, the collected RBC ghosts were extruded serially through 400 nm, 200 nm and 100 nm polycarbonate porous membranes using a mini extruder (Avanti Polar Lipids) to form RBCG. The hydrodynamic diameter and zeta potential of the RBCG were measured by DLS. The size and morphology of the RBCG were characterized by H-7650 transmission electron microscopy (HITACHI, Japan).

Preparation and Characterization of RBCG@AECho. Firstly, the collected RBC ghosts were extruded serially through 400 nm and 200 nm porous membranes. After that, 800 μL RBCG (100 μg/mL) were mixed with 200 μL AECho (0.8 mg/mL) (RBCG was determined by BCA), and then they were coextruded through a 100 nm porous membrane. The mechanical force and membrane fluidity cooperated to facilitate the AECho to cross the lipid bilayers and load into RBCG. The extrusion process was repeated for 10 times to prepare RBCG@AECho with uniform size. Finally, the product was purified with centrifugal filters (Centrifugal filter devices, 50 kD, Millipore) and washed with PBS to remove the excessive AECho. The size and morphology of RBCG@AECho were characterized by H-7650 transmission electron microscope (HITACHI, Japan). The hydrodynamic diameter and zeta potential of the RBCG@AECho were measured by DLS.

Preparation and Characterization of DBCO-RBCG@ICG. The preparation RBCG@ICG was similar to that of RBCG@AECho by mixxing 200 μL ICG (0.77 mg/mL) into 800 μL RBCG (100 μg/mL) solution before extrusion. The resulted RBCG@ICG was ultrafiltrated and washed with PBS to remove free ICG and then mixed with 100 μM NHS-PEG_4-DBCO at 37 °C for 2 h. The product was purified with centrifugal filters (Centrifugal filter devices, 100 kD, Millipore) to remove free NHS-PEG_4-DBCO. The size and morphology of DBCO-RBCG@ICG were characterized by H-7650 transmission electron microscope (HITACHI, Japan). The hydrodynamic diameter and zeta potential of the DBCO-RBCG@ICG were measured by DLS.

To verify the successful loading of ICG, the absorption spectra and flow cytometry analysis of RBCG and RBCG@ICG were obtained with a U-3900 spectrophotometer (HITACHI) and BECKMAN COULTER (Cytoflex LX), respectively.

To verify the reaction capability of DBCO on the particles by fluorescence imaging, the RBCG and DBCO-RBCG were individually fixed on glass bottom dishes at 37 °C for 1 h and then washed with PBS, followed by incubation with Azide-Flour 488 (10 μM) for 1 h. After which, the nanoparticles were viewed by confocal laser scanning microscopy (CLSM, UltraVIEW VoX, PerkinElmer, USA).

The successful preparation of DBCO-RBCG@ICG was analyzed by flow cytometry.

***In Vitro* Metabolic Incorporation Capability of RBCG@AECho.** MDA-MB-231 cells were seeded in glass bottom dishes (5×10^3 cells/well) and incubated for 24 h. After removing the medium, the cells were incubated with RBCG@AECho (100 μM AECho) at 37 °C for 1 h. Then they were washed using PBS and labeled with 10 μM DBCO-Flour 525. After that, the cells were fixed with 4% (w/v) paraformaldehyde and the nuclei were stained with Hoechst 33342. Then the cells were imaged by CLSM. Hoechst 33342 was excited with UV, emitting 450-500 nm fluorescence. The DBCO-Flour 525 was excited using a 488 nm laser, and emission was collected in the range of 510-550 nm.

***In Vivo* Metabolic Incorporation Capability of RBCG@AECho.** The Balb/c nude mice with MDA-MB-231 tumor were intratumorally (i.t.) injected of Cy7 labeled RBCG (20 μL, 10 mg/kg RBCG, RBCG was determined by BCA). Imaging analysis was taken at different time intervals using the *ex/in vivo* imaging system (FX Pro, Kodak, Japan) with a 730 nm excitation and a 790 nm filter to collect the fluorescence signal of Cy7. In the *ex-vivo* imaging experiments, the mice were sacrificed at 24 h post-injection. The tumors and major organs were collected and imaged.

To further investigate the metabolic incorporation of RBCG@AECho, three groups of MDA-MB-231 tumor-bearing mice were i.t. injected with PBS, AECho, and RBCG@AECho, respectively. After 24 h treatment, the dissected tumors and organs were frozen in optimum cutting temperature (OCT) tissue compound (Sakura, Tokyo, Japan) on dry ice and sectioned into 10 μm slices. All sections were stained serially with 10 μM DBCO-Flour 525 for 1 h and Hoechst 33342 for 15 min. The fluorescence images were acquired on a laser scanning confocal microscope (Leica TCS SP5).

Toxicity Evaluation. MDA-MB-231 cells were seeded in 96-well plates (5×10^3 cells/well) and incubated for 24 h. After which, the cells were individually incubated

with different concentrations of RBCG, RBCG@AECho, RBCG@ICG, and DBCO-RBCG@ICG for 24 h, then washed with PBS. Cell viability was determined using standard CCK-8 (Beyotime, China) assay.

***In Vitro* Specific Binding of DBCO-RBCG@ICG to RBCG@AECho Treated Cells.** MDA-MB-231 cells were seeded at a density of 5×10^4 cells per well in glass bottom dishes and incubated for 24 h. After removing the medium, the cells were incubated with DMEM or RBCG@AECho for 24 h. Then they were being washed with PBS and incubated with RBCG@ICG or DBCO-RBCG@ICG (ICG: 10 μg/mL) for 1 h at 37 °C. For microscopy imaging, the nuclei were stained with Hoechst 33342 and imaged by CLSM. ICG was excited using a 633 nm laser, and the emission was collected by photomultiplier tubes in the range of 700-800 nm. For flow cytometry analysis, the treated cells were collected and analyzed by flow cytometry and the corresponding data analysis was performed using FlowJo software.

***In Vitro* Photothermal Therapy.** MDA-MB-231 cells were seeded at a density of 1×10^5 cells per well in glass bottom dishes and incubated for 24 h. Then the cells were incubated with RBCG@AECho for 24 h. After being washed with PBS, the cells were incubated with RBCG@ICG or DBCO-RBCG@ICG (ICG: 10 μg/mL) for 1 h at 37 °C. After which, the cells were rinsed again with PBS and added 100 μL fresh culture medium, followed with illumination by an 808 nm laser (1.5 W/cm^2, 10 min) and subsequently incubated for another 4 h. Then they were stained with calcein-AM and PI for visualization of live cells and dead cells, respectively. After rinsing again with Dulbecco's Phosphate Buffered Saline (DPBS), the cells were imaged. The standard CCK-8 assay was also used to evaluate the cell viability after the cells were treated as above and incubated for another 24 h.

***In Vivo* Evaluation of the SPPAC-Based Two-Step Tumor-Targeting Strategy.** MDA-MB-231 tumor-bearing mice were randomly divided into two groups (3 per group) and injected (i.t.) with RBCG@AECho (20 μL, 10 mg/kg RBCG). 24 h later, the mice were intravenously injected with RBCG@ICG or DBCO-RBCG@ICG (100 μL, ICG: 1 mg/kg), respectively. Fluorescence (FL) imaging analysis of ICG was taken at different time intervals using the *ex/in vivo* imaging system (FX Pro, Kodak, Japan) with a 790 nm excitation wavelength and an 830 nm filter to collect the FL signals. The mice were sacrificed at 48 h post-injection. The tumors and major organs were collected and subjected for *ex vivo* imaging and semi-quantitative biodistribution analysis.

***In Vivo* Thermal Imaging.** MDA-MB-231 tumor-bearing mice were randomly divided into three groups (3 per group) and injected (i.t.) with RBCG@AECho (20 μL, 10 mg/kg RBCG). 24 h later, the mice were intravenously injected with PBS, RBCG@ICG or DBCO-RBCG@ICG (100 μL, ICG: 1 mg/kg), respectively. At 48 h post-injection of RBCG@AECho, the tumors were irradiated by an 808 nm laser at 1.5 W/cm^2 for 5 min and infrared thermographic maps were obtained by using an infrared thermal imaging camera.

Apoptosis Detection. To detect the apoptosis of tumor cells in tumor tissues, tumors were collected at 12 h post-irradiation, and then sectioned into 10 μm slices for haematoxylin and eosin (H&E) staining. Besides, the proliferation of tumor cells was measured by Ki 67 Kit. All slices were imaged by automatic multispectral imaging

system (PerkinElmer Vectra II, USA).

***In Vivo* Photothermal Therapy.** MDA-MB-231 tumor-bearing mice were randomly divided into four groups (6 per group) and injected (i.t.) with RBCG@AECho (20 μL, 10 mg/kg RBCG). At 24 h post-injection, the mice were intravenously injected with (1) PBS, (2) RBCG@ICG, (3) DBCO-RBCG@ICG or (4) DBCO-RBCG@ICG (100 μL, ICG: 1 mg/kg), respectively. At 48 h post-injection of RBCG@AECho, the tumors except in group 3 were irradiated by an 808 nm laser (1.5 W/cm^2, 8 min). The tumor volumes and body weight changes of each mouse were recorded every other day.

Statistical Analysis: Statistical analysis of the data was performed using the Student's test. All results were expressed as mean ± standard error unless otherwise noted.

Table S1. Hydrodynamic diameters and zeta potentials of RBCG, RBCG@AECho, RBCG@ICG and DBCO-RBCG@ICG. All nanoparticles showed similar average hydrodynamic diameters and zeta potentials, indicating that the AECho or ICG loading as well as DBCO modification didn't influence the hydrodynamic diameter and zeta potentials of nanoparticles. The results were expressed as the mean ± s.d (n = 3).

Sample	d (nm)	Zeta Potential (mV)	PDI
RBCG	125.8±8.1	-24.9±1.5	0.147±0.021
RBCG@AECho	129.7±3.3	-25.3±2.4	0.126±0.018
RBCG@ICG	121.9±7.8	-23.5±1.8	0.114±0.013
DBCO-RBCG@ICG	127.4±5.6	-21.9±2.1	0.212±0.054

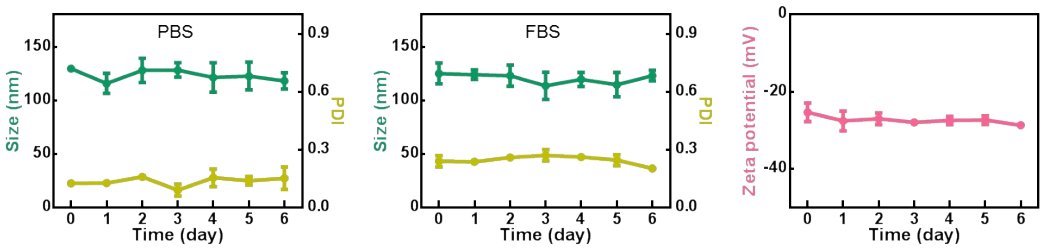

Figure S1. Size, polydispersity index (PDI) and zeta potential of RBCG@AECho in PBS or 10% FBS over 6 days. All the results indicated the good stability of RBCG@AECho in physiological environment.

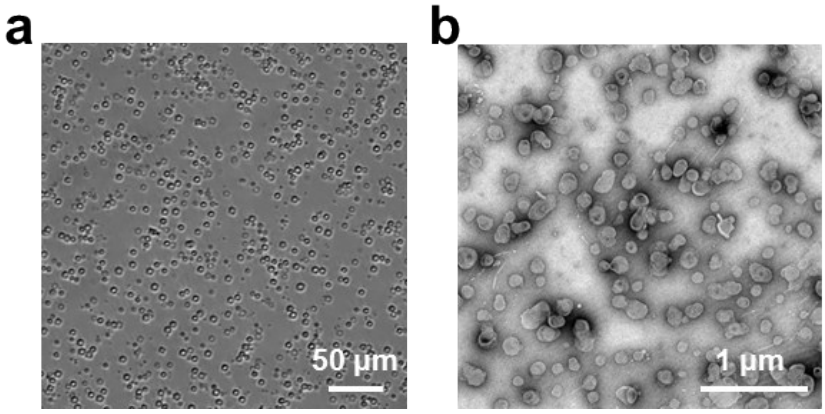

Figure S2. The microscopy image (a, before extrusion) and TEM image (b, after extrusion) of RBCG.

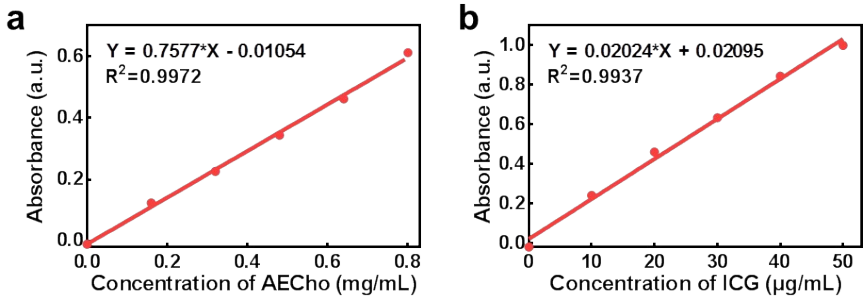

Figure S3: UV-vis standard curve of AECho (a) and ICG (b).

To determine the encapsulation efficiency of AECho, the RBCG solution (100 μg/mL, 800 μL) was mixed with AECho (0.8 mg/mL, 200 μL) and coextruded through a 100 nm porous membrane. After ultrafiltration and washed with PBS, the filtrates containing redundant AECho were collected and the absorbance value at 281 nm was measured by UV-Vis spectroscopy to quantify the AECho using UV-vis calculation curve. The encapsulation efficiency of AECho was calculated to be 8.3% by using equation:

$$\%EE = \frac{Total\ amount\ of\ AECho - Amount\ of\ AECho\ in\ filtrates}{Total\ amount\ of\ AECho} \times 100\%$$

To determine the ICG loading efficacy, the RBCG solution (100 μg/mL, 800 μL) was mixed with ICG (0.77 mg/mL, 200 μL) and coextruded through a 100 nm porous membrane. After purified with centrifugal filters (Centrifugal filter devices, 50 kD, Millipore) and washed with PBS, the filtrates containing surplus ICG was collected, and then the absorbance value at 808 nm was measured by UV-Vis spectroscopy to acquire the ICG quantity according to the UV-vis calculation curve. The loading efficacy was calculated to be 27.1% by using equation:

$$ICG\ Loading\ (\%) = \frac{Total\ amount\ of\ ICG - Amount\ of\ ICG\ in\ supernatant}{Total\ amount\ of\ RBCG@ICG} \times 100\%$$

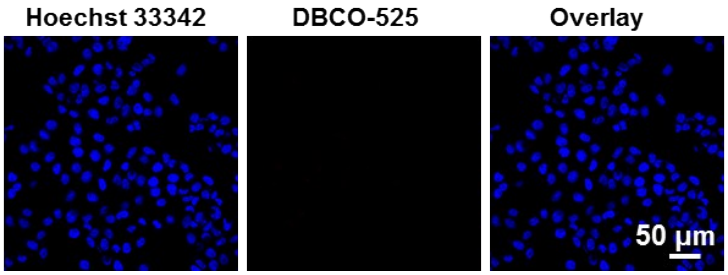

Figure S4. CLSM imaging of MDA-MB-231 cells incubated with RBCG mixed with AECho without co-extrusion, followed by DBCO-Flour 525 treatment (Blue: Hoechst 33342, red: DBCO-Flour 525).

In this experiment, 800 μL RBCG (100 μg/mL) were mixed with 200 μL AECho (0.8 mg/mL) without co-extrusion. After removing free AECho by ultrafiltration and washing, the collected RBCG was added to MDA-MB-231 cells, followed by confocal laser scanning microscope (CLSM) imaging to detect the cell-surface N_3 groups using DBCO-Flour 525. No fluorescent signal was observed on cell surface, indicating that AECho could not be loaded into RBCG without co-extrusion.

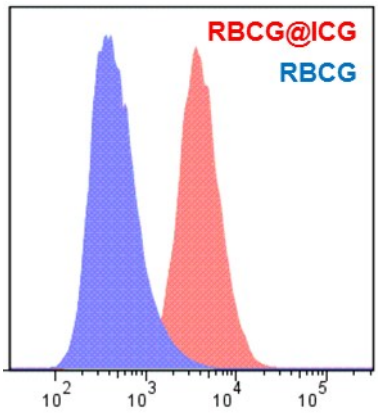

Figure S5. Flow cytometry analysis of RBCG and RBCG@ICG.

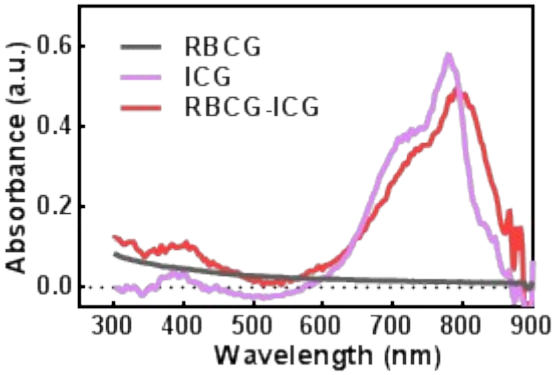

Figure S6. UV/vis absorption spectra of RBCG, free ICG and RBCG@ICG. The absorption of ICG was well maintained in RBCG@ICG.

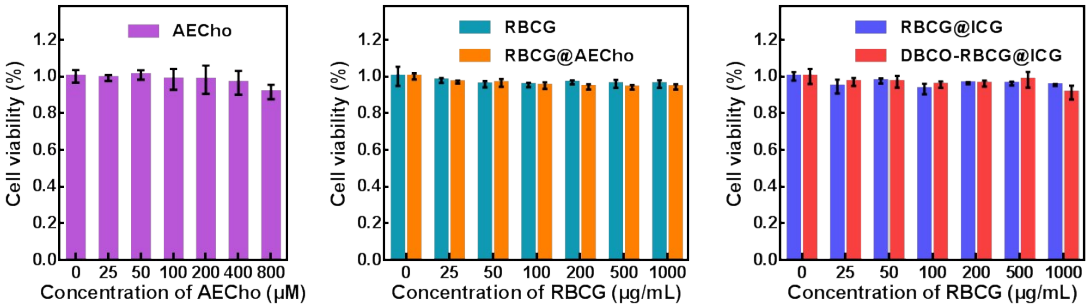

Figure S7. Cytotoxicity of AECho, RBCG, RBCG@AECho, RBCG@ICG and DBCO-RBCG@ICG against MDA-MB-231 cells. No obvious decrease in cell viability was observed in all groups, indicating the good biocompatibility of the AECho and nanoparticles. The results were expressed as the mean ± s.d (n = 3).

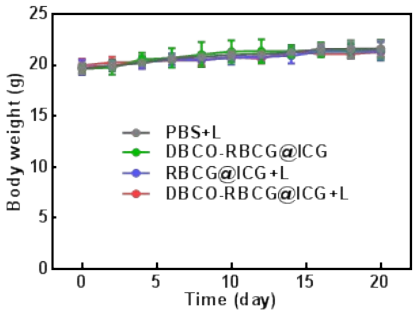

Figure S8. Body weight of MDA-MB-231 tumor-bearing mice receiving different treatments. The changes in body weight were not obvious for all groups. The results were expressed as the mean ± s.d (n = 6)

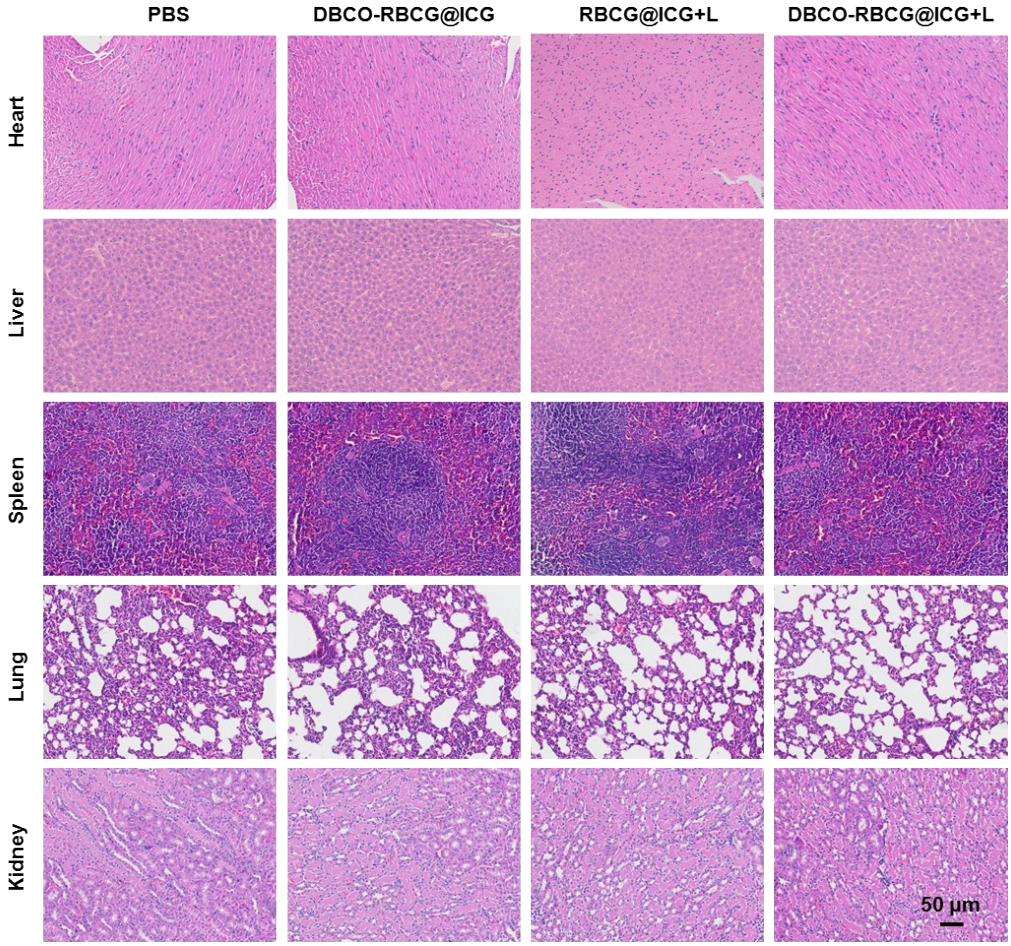

Figure S9. Representative H&E staining images of major organs in different groups. No histological abnormalities in major organs were found (heart, liver, spleen, lung and kidney).

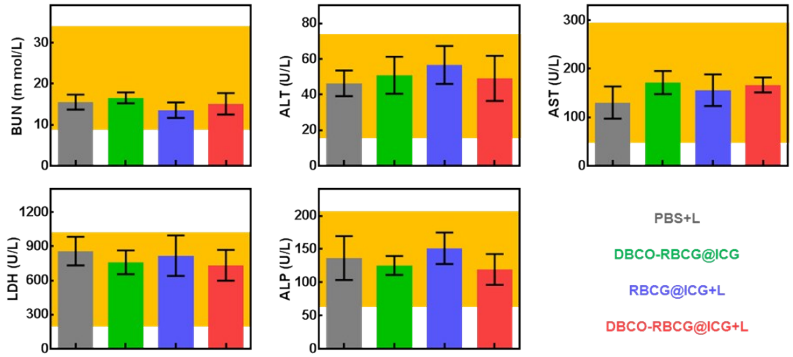

Figure S10. Blood biochemical analysis of mice after having receiving different treatments. The results were all within normal ranges, indicating the good biocompatibility of our two-step tumor-targeting. The results were expressed as the mean ± s.d (n = 6).

Abbreviations: BUN: blood urea nitrogen; ALT: alanine aminotransferase; AST: aspartate aminotransferase; ALP: alkaline phosphatase; LDH: lactate dehydrogenase.